

IConFace: Identity-Structure Asymmetric Conditioning for Unified Reference-Aware Face Restoration

Axi Niu*, Jinyang Zhang*, Senyan Qing

Northwestern Polytechnical University
 nax@nwpu.edu.cn zhangjinyang@mail.nwpu.edu.cn qingsenyan@nwpu.edu.cn
 Homepage: <https://cosmicrealm.github.io/IConFace/>

Abstract

Blind face restoration is highly ill-posed under severe degradation, where identity-critical details may be missing from the degraded input. Same-identity references reduce this ambiguity, but mismatched pose, expression, illumination, age, makeup, or local facial states can lead to overuse of reference appearance. We propose **IConFace**, a unified reference-aware and no-reference framework with identity–structure asymmetric conditioning. References are distilled into a norm-weighted global AdaFace identity anchor for image-only modulation, while the degraded image is reinforced as the spatial structure anchor through low-rank residuals and block-wise degraded cross-attention with two-route memory. The resulting single checkpoint exploits references when available and falls back to no-reference restoration when absent, improving identity consistency, fine-detail recovery, and degraded-only restoration quality in a unified model.

Introduction

Blind face restoration (BFR) recovers high-quality faces from low-quality observations with unknown degradations. Modern generative, codebook, transformer, and diffusion priors improve perceptual realism (Menon et al. 2020; Yang et al. 2021; Wang et al. 2021; Gu et al. 2022; Zhou et al. 2022; Wang et al. 2022, 2023; Zhao et al. 2023; Qiu et al. 2023; Yang et al. 2023; Lin et al. 2024; Miao et al. 2025; Wang et al. 2025), but no-reference restoration remains highly ill-posed: severe degradation can remove identity-critical evidence and local facial cues, so a plausible restoration may still drift from the target identity.

Same-identity reference images reduce this ambiguity by providing identity evidence unavailable in the degraded input (Li et al. 2018, 2020b, 2022; Hsiao et al. 2024; Liu et al. 2025; Chong et al. 2025; Yin et al. 2026). This makes reference-aware restoration useful for personal photo enhancement and legacy portrait restoration. However, references are not pure identity carriers: they also encode pose, illumination, expression, age, makeup, and local facial states. Direct transfer or over-attention to reference features may therefore improve identity similarity while overusing reference-specific appearance and failing to preserve the structure implied by the degraded input. Fig. 1 focuses on the

*These authors contributed equally.



Figure 1: **Teaser comparison.** IConFace preserves reference-consistent facial details better than strong blind and reference-aware baselines while remaining anchored to the degraded input.

complementary detail-recovery challenge: competing methods may produce plausible faces while suppressing or distorting identity-related local details.

Practical systems must also handle missing references. Same-identity references may be abundant, limited, noisy, or entirely absent. Existing blind methods lack explicit identity evidence, while many reference-aware methods rely on matching, alignment, personalization, or memory transfer that is less natural in the no-reference case. A useful model should exploit references when available and fall back to robust degraded-only restoration when they are absent.

We propose **IConFace**, a unified framework based on asymmetric identity–structure conditioning. References are compressed into a global identity controller, while the degraded image remains the spatial structure anchor. A hybrid concat backbone keeps degraded and reference tokens as visual evidence, and two lightweight side pathways ex-

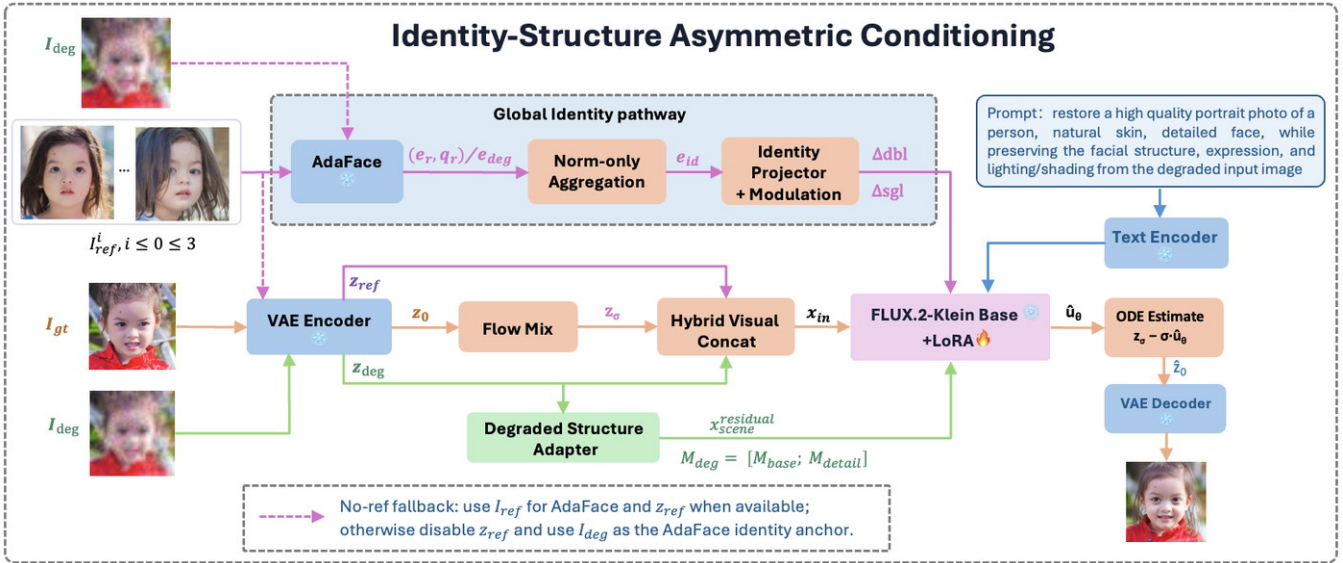


Figure 2: Overview of **IConFace**. The main route keeps the hybrid concat sequence $x_{in} = [x_{scene}; x_{deg}; x_{ref}]$ in the restoration backbone. A global identity pathway compresses references into a single AdaFace anchor and injects image-only modulation. A degraded structure pathway reinforces the degraded observation with a low-rank input residual and block-wise degraded cross-attention using two-route pooled memory for base structure anchor and local detail. When references are absent, $x_{ref} = \emptyset$ and the identity pathway falls back to a degraded-image AdaFace anchor as weak self-conditioning.

explicitly control identity and structure. This design improves reference-aligned identity consistency and fine-detail recovery under severe degradation while preserving no-reference restoration capability.

Contributions. Our contributions are:

- A unified optional-reference formulation where one checkpoint supports reference-aware and no-reference restoration through asymmetric identity–structure conditioning.
- Lightweight pathways that use norm-weighted AdaFace modulation for reference identity and low-rank residuals with two-route degraded memory for structure and detail anchoring.
- Extensive results showing improved reference-aligned identity consistency, fine-detail recovery under severe degradation, and strong no-reference perceptual quality.

Related Work

Blind face restoration. Blind and real-world restoration have evolved from geometric priors to degradation modeling, generative priors, dictionaries, codebooks, transformers, and diffusion models (Li et al. 2020a; Yang et al. 2020, 2021; Wang et al. 2021; Gu et al. 2022; Zhou et al. 2022; Wang et al. 2022, 2023; Zhao et al. 2023; Qiu et al. 2023; Yang et al. 2023; Lin et al. 2024; Tsai et al. 2024; Miao et al. 2025; Wang et al. 2025; Niu et al. 2025, 2023, 2024; Li et al. 2025). These methods improve realism, but degraded-only evidence remains ambiguous under strong corruption.

Reference-aware restoration and conditioning. Reference-guided restoration uses exemplars to recover identity cues through warping, adaptive fusion, memory

dictionaries, latent diffusion conditioning, or personalized adapters (Li et al. 2018, 2020b, 2022; Varanka et al. 2024; Hsiao et al. 2024; Ying et al. 2024; Zhang et al. 2024; Liu et al. 2025; Chong et al. 2025; Yin et al. 2026). These works show the value of references, but references also carry pose, expression, illumination, and local states that may not match the target. **IConFace** is also related to broader conditioning and control mechanisms (Vaswani et al. 2017; Rombach et al. 2022; Peebles and Xie 2023; Meng et al. 2022; Zhang, Rao, and Agrawala 2023; Ye et al. 2023; Yan et al. 2019, 2020); auxiliary evidence is most useful when its role is explicit. We specialize this principle by distilling references into a global identity anchor while reinforcing the degraded image as the spatial structure anchor.

Method

Problem Setup

Given a degraded face image I_{deg} and an optional set of same-identity references $\mathcal{R} = \{I_{ref}^1, \dots, I_{ref}^N\}$, our goal is to generate a restored image \hat{I} that preserves the structure and facial state implied by I_{deg} . When references are available, the model should additionally recover reference-consistent identity cues and fine details. When $\mathcal{R} = \emptyset$, it should operate as a no-reference blind restorer.

We train in latent space with a flow-matching objective. Given clean latent z_0 , noise $\epsilon \sim \mathcal{N}(0, I)$, and noise level $\sigma \in [0, 1]$, we form

$$z_\sigma = (1 - \sigma)z_0 + \sigma\epsilon, \quad u^* = \epsilon - z_0. \quad (1)$$

The restoration network predicts $\hat{u}_\theta = f_\theta(z_\sigma, I_{deg}, \mathcal{R}, \sigma)$ and recovers $\hat{z}_0 = z_\sigma - \sigma\hat{u}_\theta$.

Overview of IConFace

IConFace is built on the FLUX.2-klein-base-4B hybrid concat restoration backbone. The main sequence concatenates noisy scene tokens, degraded-image tokens, and optional reference tokens:

$$x_{\text{in}} = [x_{\text{scene}}; x_{\text{deg}}; x_{\text{ref}}]. \quad (2)$$

In no-reference mode, $x_{\text{ref}} = \emptyset$ and the same degraded-conditioned backbone is retained. IConFace augments this backbone with two side pathways: a global identity pathway that aggregates references into a single AdaFace identity anchor, and a degraded structure pathway that reinforces the spatially aligned degraded observation.

Asymmetric Identity–Structure Conditioning

The central design principle of IConFace is that degraded and reference observations should not be treated symmetrically. The degraded image is the only observation spatially aligned with the target image, so it should remain the structure anchor. References are valuable identity evidence, but they also contain pose, expression, illumination, makeup, age, and local facial states that should not be copied indiscriminately. IConFace therefore assigns references a global identity-control role and assigns degraded tokens a structure-preserving role.

This asymmetry is implemented through three choices. First, the hybrid concat backbone remains the main carrier of degraded and reference evidence. Second, references are aggregated into a single global AdaFace identity anchor for image-only modulation when they are available. Third, degraded tokens are reinforced through an explicit low-rank residual and block-wise degraded memory. In no-reference operation, the reference segment is removed rather than replaced by duplicated placeholders, and the identity pathway uses the degraded-image AdaFace fallback only as weak forward conditioning.

Global Identity Pathway

For each valid reference I_{ref}^r , frozen AdaFace returns a raw embedding $z_r \in \mathbb{R}^{512}$. We separate identity direction and reliability:

$$e_r = z_r / \|z_r\|_2, \quad q_r = \|z_r\|_2. \quad (3)$$

The norm q_r acts as a quality proxy. With temperature T , multiple references are aggregated by norm-only weights:

$$w_r = \text{softmax}(\log q_r / T), \quad e_{\text{ref}} = \text{Norm} \left(\sum_r w_r e_r \right). \quad (4)$$

If references are absent, the pathway falls back to the normalized AdaFace embedding of I_{deg} . This fallback is used only as weak forward conditioning, not as a reference supervision target.

The effective identity anchor e_{id} is projected into the backbone hidden space and transformed into modulation deltas for double-stream and single-stream image blocks:

$$h_{\text{id}} = \phi_{\text{global}}(e_{\text{id}}), \quad \Delta_{\text{dbl}}, \Delta_{\text{sgl}} = \psi_{\text{dbl}}(h_{\text{id}}), \psi_{\text{sgl}}(h_{\text{id}}). \quad (5)$$

The deltas are applied only to image tokens; the text stream is untouched. This gives references a global identity-control role without turning them into a local structure-transfer branch.

Degraded Structure Pathway

The degraded image is the only observation spatially aligned with the target, so IConFace reinforces it as the structure anchor. First, degraded tokens resized to the scene-token resolution are injected through a low-rank input residual:

$$x_{\text{scene}}^{\text{residual}} = s_{\text{deg}} W_{\text{in}}(\tilde{x}_{\text{deg}}), \quad (6)$$

$$x'_{\text{scene}} = x_{\text{scene}} + x_{\text{scene}}^{\text{residual}}.$$

Second, full degraded attention is compressed into a fixed memory budget by two learned-query poolers. A base route pools x_{deg} to preserve global layout and illumination, while a detail route pools $x_{\text{deg}} - \text{smooth}(x_{\text{deg}})$ to emphasize local facial cues:

$$M_{\text{base}} = P_b(x_{\text{deg}}),$$

$$M_{\text{detail}} = P_d(x_{\text{deg}} - \text{smooth}(x_{\text{deg}})), \quad (7)$$

$$M_{\text{deg}} = [M_{\text{base}}; M_{\text{detail}}],$$

$$h'_\ell = h_\ell + \gamma_\ell \text{Attn}(Q_\ell h_\ell, K_\ell M_{\text{deg}}, V_\ell M_{\text{deg}}).$$

Here P_b and P_d are learned-query poolers, h_ℓ denotes image tokens in block ℓ , and the K/V projectors are low-rank. The adapter therefore outputs both the scene residual and the two-route degraded memory. This additive image-only path lets each block read both coarse degraded structure and high-frequency degraded detail without replacing the main concat route.

Training Objective

The main restoration loss regresses the flow field:

$$\mathcal{L}_{\text{fm}} = \mathbb{E}_{z_0, \epsilon, \sigma} [w(\sigma) \|\hat{u}_\theta - (\epsilon - z_0)\|_2^2]. \quad (8)$$

In the final model, the flow-matching timestep weight is uniform, i.e., $w(\sigma) = 1$; only the identity loss below uses sigma-dependent weighting. For reference-aware training samples, we decode the current clean-latent estimate \hat{z}_0 and compute a frozen-AdaFace identity loss against the reference anchor:

$$\mathcal{L}_{\text{ref-id}} = 1 - \cos(A(\hat{I}), \text{sg}(e_{\text{ref}})), \quad (9)$$

where $A(\cdot)$ is the frozen AdaFace encoder and sg stops gradients through the target. We also use a weak clean-target stabilizer

$$\mathcal{L}_{\text{hard}} = 1 - \cos(A(\hat{I}), \text{sg}(e_{\text{gt}})) \quad (10)$$

for imperfect references. The sigma-weighted identity objective is

$$\mathcal{L}_{\text{id}} = \omega(\sigma) [(1 - \lambda_h^*) \mathcal{L}_{\text{ref-id}} + \lambda_h^* \mathcal{L}_{\text{hard}}], \quad (11)$$

where $\lambda_h^* = \lambda_h (1 - \cos(e_{\text{ref}}, e_{\text{gt}}))$ increases the stabilizer weight when the selected reference is less consistent with the clean target. We use $\omega(\sigma) = \max(1 - \sigma, \omega_{\text{min}})^2$ with $\omega_{\text{min}} = 0.25$, so high-noise steps are down-weighted rather than hard-skipped. For no-reference samples, $\mathcal{L}_{\text{id}} = 0$ because no reference identity target exists. The final loss is

$$\mathcal{L} = \mathcal{L}_{\text{fm}} + \lambda_{\text{id}} \mathcal{L}_{\text{id}}. \quad (12)$$

Additional implementation details are provided in the supplementary material.

Table 1: Reference-aware restoration on CelebA-Test-Ref, FFHQ-Ref Moderate, FFHQ-Ref Severe, and CelebHQRef100. Ref metrics are computed against the first protocol reference.

Method	Dataset	Ref-ArcFace \uparrow	Ref-AdaFace \uparrow	MUSIQ \uparrow	CLIP-IQA \uparrow	MANIQA \uparrow
DMDNet	CelebA-Test-Ref	0.472	0.471	72.725	0.625	0.495
ReF-LDM		0.573	0.569	74.426	0.675	0.527
RestorerID		0.539	0.530	72.820	0.695	0.536
InstantRestore		0.533	0.534	71.324	0.555	0.494
FaceMe		0.544	0.542	70.716	0.586	0.480
Ours		0.655	0.658	76.068	0.727	0.635
DMDNet	FFHQ-Ref Moderate	0.572	0.564	72.024	0.633	0.477
ReF-LDM		0.641	0.629	75.254	0.708	0.544
RestorerID		0.605	0.590	72.111	0.690	0.509
InstantRestore		0.604	0.599	69.358	0.568	0.463
FaceMe		0.640	0.629	72.480	0.610	0.491
Ours		0.701	0.689	76.220	0.738	0.613
DMDNet	FFHQ-Ref Severe	0.137	0.127	62.177	0.543	0.355
ReF-LDM		0.595	0.588	75.744	0.717	0.552
RestorerID		0.425	0.407	73.602	0.708	0.536
InstantRestore		0.473	0.477	69.998	0.581	0.467
FaceMe		0.457	0.455	72.251	0.610	0.493
Ours		0.701	0.692	75.679	0.726	0.600
DMDNet	CelebHQRef100	0.379	0.370	70.529	0.604	0.465
ReF-LDM		0.577	0.567	75.214	0.695	0.558
RestorerID		0.459	0.430	73.228	0.712	0.549
InstantRestore		0.510	0.507	70.671	0.581	0.496
FaceMe		0.451	0.437	72.245	0.618	0.524
Ours		0.700	0.700	75.673	0.729	0.625

Reference-aware qualitative comparisons

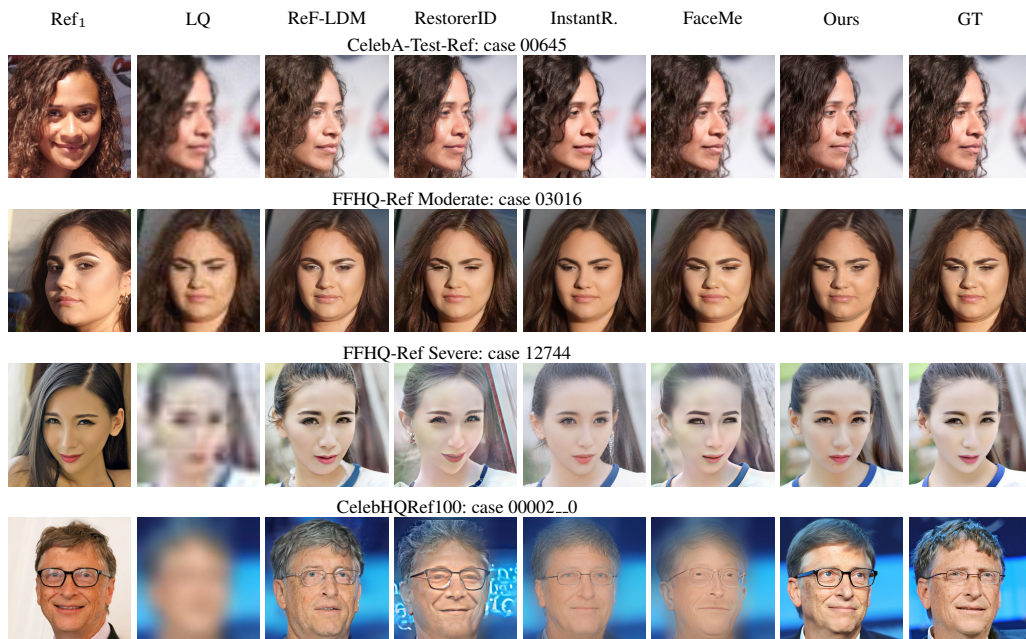


Figure 3: Reference-aware qualitative comparisons across four benchmarks. Each row shows Ref₁, LQ, method outputs, and GT under the same protocol references. IConFace keeps reference-consistent details while preserving the degraded facial structure.

Experiments

Experimental Setup

We train on FFHQ-Ref with online mixed blind degradations combining Real-ESRGAN and BSRGAN style degradation

operators, and evaluate a single checkpoint in two modes. FFHQ-Ref train is used for training, while FFHQ-Ref val is used only for preview and qualitative validation. To expose the same model to varying reference availability, train-

ing samples use a mixed protocol: 30% without references, 30% with one reference, 20% with two references, and 20% with three references. When fewer references are available, we use the actual number without duplication.

Reference-aware benchmarks include CelebA-Test-Ref (2,533 samples), FFHQ-Ref Moderate (857), FFHQ-Ref Severe (857), and CelebHQRef100 (100 identities). No-reference benchmarks include CelebA-Test (3,000), LFW (1,711), CelebChild (360), WebPhoto (407), and Wider-Test (970). Reference-aware baselines include DMDNet, ReFLDM, RestorerID, InstantRestore, and FaceMe (Li et al. 2022; Hsiao et al. 2024; Ying et al. 2024; Zhang et al. 2024; Liu et al. 2025); blind baselines include CodeFormer, VQFR, GFP-GAN, RestoreFormer++, and DAEFR (Zhou et al. 2022; Gu et al. 2022; Wang et al. 2021, 2023; Tsai et al. 2024).

All reported IConFace results use the same checkpoint with 12 sampling steps and the same restoration prompt in both modes. In reference-aware mode, up to three same-identity references are provided. In no-reference mode, reference tokens are absent and the identity pathway uses the degraded-image AdaFace fallback only as weak self-conditioning. For no-reference benchmarks, including real-world sets without paired ground truth, we report learned no-reference perceptual metrics.

CelebHQRef100 is used as a compact diagnostic split for severe same-identity reference transfer; its construction details are provided in the supplementary material. CelebA-Test provides paired synthetic degraded/GT portraits for degraded-only evaluation, while LFW, CelebChild, WebPhoto, and Wider-Test are real-world no-reference sets without paired targets. We therefore do not mix reference-aware and no-reference baselines in a single aggregate ranking; each method is evaluated in its intended inference mode, and the two result blocks answer separate protocol-specific restoration questions.

Reference-Aware Restoration

Reference-aware identity evaluation should separate reference utilization from paired target-state matching. Protocol references and GT targets are same-identity images but may differ in pose, expression, illumination, age, makeup, or local facial state; on CelebA-Test-Ref, 49.11% and 80.77% of Ref₁-GT pairs fall below AdaFace 0.6 and 0.7, respectively (supplementary Table 2). We therefore use Ref-AdaFace, supported by Ref-ArcFace, as the primary reference-aware identity measure, and report GT-AdaFace and structure checks in the supplement.

Table 1 reports reference-aware restoration results. IConFace achieves the best Ref-ArcFace and Ref-AdaFace on all four benchmarks, with especially large gains on FFHQ-Ref Severe and CelebHQRef100 where degraded identity evidence is weak. IConFace is also consistently strong on MUSIQ, CLIP-IQA, and MANIQA, supporting the intended identity-structure tradeoff rather than a pure identity-score optimization. Supplementary Table 4 further shows a reversal: IConFace is not highest on GT-AdaFace in easier splits, but leads on FFHQ-Ref Severe and CelebHQRef100, indicating that the reference pathway provides genuine iden-

Table 2: No-reference restoration on LFW, CelebChild, WebPhoto, Wider-Test, and CelebA-Test.

Method	Dataset	MUSIQ \uparrow	CLIP \uparrow	MANIQA \uparrow
CodeFormer	LFW	75.484	0.689	0.527
GFP-GAN		75.570	0.676	0.551
VQFR		74.901	0.725	0.543
RF++		72.251	0.702	0.511
DAEFR		75.840	0.697	0.542
Ours		76.712	0.758	0.645
CodeFormer	CelebChild	74.852	0.686	0.521
GFP-GAN		74.822	0.674	0.530
VQFR		74.459	0.711	0.542
RF++		71.690	0.702	0.506
DAEFR		74.883	0.697	0.537
Ours		75.603	0.750	0.613
CodeFormer	WebPhoto	74.004	0.692	0.503
GFP-GAN		75.213	0.702	0.543
VQFR		71.602	0.690	0.502
RF++		71.487	0.695	0.490
DAEFR		72.705	0.669	0.494
Ours		75.795	0.719	0.593
CodeFormer	Wider-Test	73.407	0.699	0.496
GFP-GAN		74.769	0.700	0.550
VQFR		72.011	0.722	0.514
RF++		71.518	0.717	0.477
DAEFR		74.143	0.697	0.520
Ours		75.496	0.729	0.616
CodeFormer	CelebA-Test	75.554	0.671	0.538
GFP-GAN		75.466	0.672	0.568
VQFR		74.406	0.691	0.552
RF++		73.914	0.689	0.553
DAEFR		75.251	0.668	0.545
Ours		75.988	0.724	0.631

tity recovery when degraded evidence is missing rather than merely copying reference state.

The largest margins appear in the severe and diagnostic reference-transfer settings. On FFHQ-Ref Severe, IConFace improves Ref-AdaFace by 0.104 over the best baseline (0.692 vs. 0.588), while also giving the best CLIP-IQA and MANIQA. On CelebHQRef100, the Ref-AdaFace margin reaches 0.133 (0.700 vs. 0.567). These gains are not obtained by sacrificing perceptual quality: the method remains first or second on MUSIQ and first on CLIP-IQA/MANIQA in the severe and diagnostic splits. Fig. 3 shows the same tradeoff visually. Under moderate degradation, IConFace preserves the degraded-image structure while restoring hair contours, eyes, skin texture, mouth boundaries, and fine identity marks such as the small mole around the lower chin. Under severe degradation, where competing methods often over-smooth, collapse, or miss identity-specific details, IConFace still produces satisfactory faces with clearer reference-consistent details and a layout anchored to the low-quality input. The joint improvement of Ref-AdaFace and perceptual metrics is important: it indicates that the reference pathway supplies identity evidence without merely optimizing a recognizer score at the expense of visual fidelity.

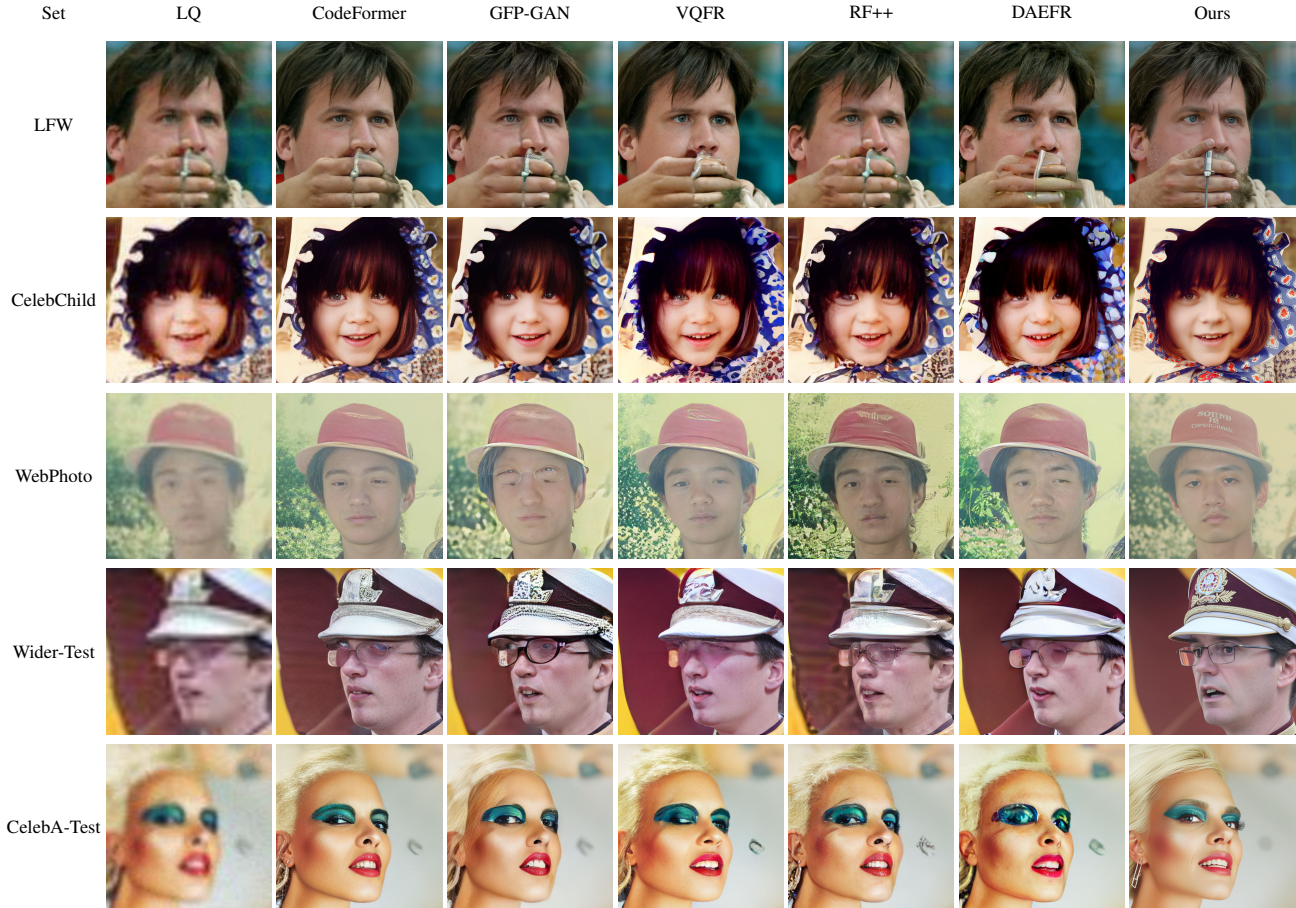


Figure 4: No-reference qualitative examples in the empty-reference mode. Each row shows one benchmark case.

No-Reference Generalization

The same checkpoint also operates without references by removing reference tokens and using the degraded-image AdaFace fallback. Table 2 shows that IConFace ranks first on MUSIQ, CLIP-IQA, and MANIQA across all five no-reference benchmarks, with average margins of 0.667 MUSIQ, 0.026 CLIP-IQA, and 0.069 MANIQA over the strongest baseline in each dataset block. The gains hold on synthetic CelebA-Test and real-world LFW, CelebChild, WebPhoto, and Wider-Test, indicating that reference-aware training does not over-specialize the model to reference-conditioned inputs. Fig. 4 further shows clearer and more realistic eyes, reasonable recovery of nearby hands or context when present, sharper facial boundaries, and stable visual quality under unknown degradations where other methods may fail or produce unstable facial details.

Implementation Details

IConFace is trained at 512 resolution using the FLUX.2-klein-base-4B restoration backbone with rank 16 LoRA adapters. Online degradations mix Real-ESRGAN and BSRGAN style degradation operators so that the model sees both common synthetic corruptions and stronger blind-restoration artifacts. The global identity pathway uses AdaFace IR50 embeddings with norm-only multi-reference

aggregation and temperature 1.0. The degraded structure pathway uses low-rank degraded cross-attention with 256 compressed memory tokens, split into base and detail routes. Training mixes samples with zero, one, two, or three references, so the same checkpoint learns both empty-reference restoration and reference-aware restoration. All main results use guidance scale 4.0, seed 42, and 12 sampling steps.

Ablation Study

We ablate IConFace on FFHQ-Ref Moderate and FFHQ-Ref Severe to separate the two design goals: using reference identity evidence and keeping the result anchored to the degraded input. *Concat* keeps only the hybrid degraded-reference token sequence, testing whether concatenation alone can learn the identity–structure balance. *Struct* adds the degraded structure adapter, isolating the value of explicit degraded-image reinforcement. *ID* adds global AdaFace modulation, testing whether a compact identity anchor is more reliable than dense reference transfer. *1-Route* keeps both side pathways but replaces the base/detail split with one degraded-memory route, and *Full* is the complete IConFace design. The cumulative order avoids conflating module effects: it first tests implicit fusion, then explicit degraded-image reinforcement, then global identity anchoring, and finally the separation of coarse layout memory from local detail memory. This makes the comparison strictly modular.

Table 3: Reference-aware ablations on FFHQ-Ref Moderate and FFHQ-Ref Severe. Variants progressively add degraded-structure reinforcement, global identity conditioning, and two-route degraded memory. Ref metrics are computed against the first protocol reference.

Dataset	Variant	Ref-ArcFace \uparrow	Ref-AdaFace \uparrow	MUSIQ \uparrow	CLIP-IQA \uparrow	MANIQA \uparrow
FFHQ-Ref Moderate	Concat baseline	0.655	0.633	75.917	0.724	0.599
	+ degraded structure	0.656	0.636	75.980	0.733	0.606
	+ global identity	0.678	0.671	76.088	0.737	0.616
	+ single-route memory	0.683	0.681	76.135	0.736	0.611
	IConFace (full)	0.688	0.689	76.220	0.738	0.613
FFHQ-Ref Severe	Concat baseline	0.602	0.597	75.205	0.717	0.595
	+ degraded structure	0.612	0.609	75.316	0.723	0.597
	+ global identity	0.654	0.660	75.430	0.722	0.593
	+ single-route memory	0.674	0.681	75.485	0.725	0.597
	IConFace (full)	0.682	0.692	75.679	0.726	0.600

Reference-aware ablation examples

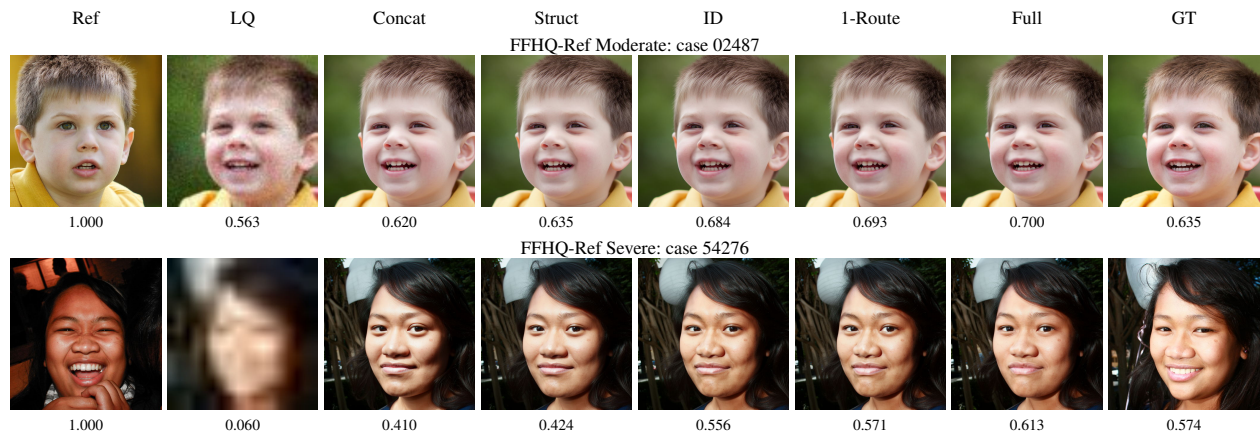


Figure 5: Reference-aware qualitative ablations on FFHQ-Ref Moderate and FFHQ-Ref Severe. Scores under crops report AdaFace similarity to the first protocol reference.

Table 3 shows that the modules play different roles. Struct gives modest but consistent gains, matching its purpose as a structure and quality stabilizer rather than an identity controller. ID gives the largest Ref-AdaFace jump, from 0.633 to 0.671 on Moderate and from 0.597 to 0.660 on Severe, showing that the global identity anchor is the main source of reference alignment. 1-Route further improves identity by letting blocks read compressed degraded evidence, but Full performs best because base memory preserves global layout while detail memory emphasizes local facial cues. Relative to Concat, Full improves Ref-AdaFace by 0.056 on Moderate and 0.095 on Severe. Fig. 5 provides a case-level view of the same ablation trend: adding the proposed modules steadily improves AdaFace similarity to the protocol reference, and the full model obtains the highest reference similarity in both examples.

Discussion and limitations. Ref metrics measure alignment to the supplied identity evidence and should be read together with visual comparisons, not as evidence of copying reference pose or expression. The results suggest that IConFace improves reference use while retaining the degraded input as the main spatial observation. This is most useful under severe degradation, where the reference provides identity evidence that the degraded image no longer

contains, but the degraded image still offers coarse structure. The method is nevertheless limited by the quality and correctness of the references, the robustness of the frozen identity encoder, and the amount of spatial evidence preserved in the degraded input. Very low-quality, occluded, or identity-inconsistent references may produce unreliable identity anchors, and extremely corrupted inputs can still leave ambiguous local details.

Conclusion. IConFace assigns references a global identity role and the degraded image a spatial-structure role. With this asymmetric design, the same checkpoint supports both reference-aware and no-reference restoration. Experiments show that the global identity pathway improves reference-aligned identity consistency, while degraded-structure reinforcement and two-route memory provide consistent gains in the ablation study. The resulting model improves severe-case identity recovery, maintains perceptual quality, and remains robust in degraded-only mode.

References

- Chong, M. J.; Xu, D.; Zhang, Y.; Wang, Z.; and Forsyth, D. 2025. Copy or Not? Reference-Based Face Image Restoration with Fine Details. In *IEEE/CVF Winter Conference on Applications of Computer Vision (WACV)*.
- Gu, Y.; Wang, X.; Xie, L.; Dong, C.; Li, G.; Shan, Y.; and Cheng, M.-M. 2022. VQFR: Blind Face Restoration with Vector-Quantized Dictionary and Parallel Decoder. In *European Conference on Computer Vision (ECCV)*, 126–143.
- Hsiao, C.-W.; Liu, Y.-L.; Yang, C.-K.; Kuo, S.-P.; Jou, Y. K.; and Chen, C.-P. 2024. ReF-LDM: A Latent Diffusion Model for Reference-based Face Image Restoration. In *Advances in Neural Information Processing Systems (NeurIPS)*.
- Li, W.; Wang, M.; Zhang, K.; Li, J.; Li, X.; Zhang, Y.; Gao, G.; Deng, W.; and Lin, C.-W. 2025. Survey on Deep Face Restoration: From Non-blind to Blind and Beyond. *ACM Computing Surveys*.
- Li, X.; Chen, C.; Zhou, S.; Lin, X.; Zuo, W.; and Zhang, L. 2020a. Blind Face Restoration via Deep Multi-scale Component Dictionaries. In *Proceedings of the European Conference on Computer Vision (ECCV)*, 399–415.
- Li, X.; Li, W.; Ren, D.; Zhang, H.; Wang, M.; and Zuo, W. 2020b. Enhanced Blind Face Restoration with Multi-Exemplar Images and Adaptive Spatial Feature Fusion. In *Proceedings of the IEEE/CVF Conference on Computer Vision and Pattern Recognition (CVPR)*, 2706–2715.
- Li, X.; Liu, M.; Ye, Y.; Zuo, W.; Lin, L.; and Yang, R. 2018. Learning Warped Guidance for Blind Face Restoration. In *Proceedings of the European Conference on Computer Vision (ECCV)*, 272–289.
- Li, X.; Zhang, S.; Zhou, S.; Zhang, L.; and Zuo, W. 2022. Learning Dual Memory Dictionaries for Blind Face Restoration. *IEEE Transactions on Pattern Analysis and Machine Intelligence*, 45(5): 5904–5919.
- Lin, X.; He, J.; Chen, Z.; Lyu, Z.; Dai, B.; Yu, F.; Qiao, Y.; Ouyang, W.; and Dong, C. 2024. DiffBIR: Toward Blind Image Restoration with Generative Diffusion Prior. In *Proceedings of the European Conference on Computer Vision (ECCV)*.
- Liu, S.; Duan, Z.-P.; Ouyang, J.; Fu, J.; Park, H.; Liu, Z.; Guo, C.; and Li, C. 2025. FaceMe: Robust Blind Face Restoration with Personal Identification. In *AAAI Conference on Artificial Intelligence*.
- Meng, C.; He, Y.; Song, Y.; Song, J.; Wu, J.; Zhu, J.-Y.; and Ermon, S. 2022. SDEdit: Guided Image Synthesis and Editing with Stochastic Differential Equations. In *International Conference on Learning Representations*.
- Menon, S.; Damian, A.; Hu, S.; Ravi, N.; and Rudin, C. 2020. PULSE: Self-Supervised Photo Upsampling via Latent Space Exploration of Generative Models. In *Proceedings of the IEEE/CVF Conference on Computer Vision and Pattern Recognition*, 2437–2445.
- Miao, Y.; Qu, Z.; Gao, M.; Chen, C.; Song, J.; Han, J.; and Deng, J. 2025. Unlocking the Potential of Diffusion Priors in Blind Face Restoration. In *Proceedings of the IEEE/CVF International Conference on Computer Vision (ICCV)*, 13471–13480.
- Niu, A.; Pham, T. X.; Zhang, K.; Sun, J.; Zhu, Y.; Yan, Q.; Kweon, I. S.; and Zhang, Y. 2024. ACDMSR: Accelerated Conditional Diffusion Models for Single Image Super-Resolution. *IEEE Transactions on Broadcasting*, 70(2): 492–504.
- Niu, A.; Zhang, K.; Pham, T. X.; Sun, J.; Zhu, Y.; Kweon, I. S.; and Zhang, Y. 2023. CDPMSR: Conditional Diffusion Probabilistic Models for Single Image Super-Resolution. In *Proceedings of the IEEE International Conference on Image Processing (ICIP)*, 615–619.
- Niu, A.; Zhang, K.; Pham, T. X.; Wang, P.; Sun, J.; Kweon, I. S.; and Zhang, Y. 2025. Learning From Multi-Perception Features for Real-World Image Super-Resolution. *IEEE Transactions on Circuits and Systems for Video Technology*, 35(7): 6535–6548.
- Peebles, W.; and Xie, S. 2023. Scalable Diffusion Models with Transformers. In *Proceedings of the IEEE/CVF International Conference on Computer Vision*, 4195–4205.
- Qiu, X.; Han, C.; Zhang, Z.; Li, B.; Guo, T.; and Nie, X. 2023. DiffBFR: Bootstrapping Diffusion Model Towards Blind Face Restoration. In *Proceedings of the 31st ACM International Conference on Multimedia*, 7785–7795.
- Rombach, R.; Blattmann, A.; Lorenz, D.; Esser, P.; and Ommer, B. 2022. High-Resolution Image Synthesis with Latent Diffusion Models. In *IEEE/CVF Conference on Computer Vision and Pattern Recognition (CVPR)*, 10684–10695.
- Tsai, Y.-J.; Liu, Y.-L.; Qi, L.; Chan, K. C.; and Yang, M.-H. 2024. Dual Associated Encoder for Face Restoration. In *International Conference on Learning Representations (ICLR)*.
- Varanka, T.; Toivonen, T.; Tripathy, S.; Zhao, G.; and Acar, E. 2024. PFStorer: Personalized Face Restoration and Super-Resolution. In *Proceedings of the IEEE/CVF Conference on Computer Vision and Pattern Recognition (CVPR)*.
- Vaswani, A.; Shazeer, N.; Parmar, N.; Uszkoreit, J.; Jones, L.; Gomez, A. N.; Kaiser, L.; and Polosukhin, I. 2017. Attention Is All You Need. In *Advances in Neural Information Processing Systems*, volume 30.
- Wang, J.; Gong, J.; Zhang, L.; Chen, Z.; Liu, X.; Gu, H.; Liu, Y.; Zhang, Y.; and Yang, X. 2025. OSDFace: One-Step Diffusion Model for Face Restoration. In *Proceedings of the IEEE/CVF Conference on Computer Vision and Pattern Recognition (CVPR)*.
- Wang, X.; Li, Y.; Zhang, H.; and Shan, Y. 2021. Towards Real-World Blind Face Restoration with Generative Facial Prior. In *IEEE/CVF Conference on Computer Vision and Pattern Recognition (CVPR)*, 9168–9178.
- Wang, Z.; Zhang, J.; Chen, R.; Wang, W.; and Luo, P. 2022. RestoreFormer: High-Quality Blind Face Restoration from Undegraded Key-Value Pairs. In *IEEE/CVF Conference on Computer Vision and Pattern Recognition (CVPR)*, 17512–17521.
- Wang, Z.; Zhang, J.; Chen, R.; Wang, W.; and Luo, P. 2023. RestoreFormer++: Towards Real-World Blind Face Restoration from Undegraded Key-Value Pairs. *IEEE Transactions on Pattern Analysis and Machine Intelligence*, 46(4): 2555–2566.

Yan, Q.; Gong, D.; Shi, Q.; van den Hengel, A.; Shen, C.; Reid, I.; and Zhang, Y. 2019. Attention-Guided Network for Ghost-Free High Dynamic Range Imaging. In *Proceedings of the IEEE/CVF Conference on Computer Vision and Pattern Recognition (CVPR)*, 1751–1760.

Yan, Q.; Zhang, L.; Liu, Y.; Zhu, Y.; Sun, J.; Shi, Q.; and Zhang, Y. 2020. Deep HDR Imaging via A Non-Local Network. *IEEE Transactions on Image Processing*, 29: 4308–4322.

Yang, L.; Wang, S.; Ma, S.; Gao, W.; Liu, C.; Wang, P.; and Ren, P. 2020. HiFaceGAN: Face Renovation via Collaborative Suppression and Replenishment. In *Proceedings of the 28th ACM International Conference on Multimedia*, 1551–1560.

Yang, P.; Zhou, S.; Tao, Q.; and Loy, C. C. 2023. PGDiff: Guiding Diffusion Models for Versatile Face Restoration via Partial Guidance. In *Advances in Neural Information Processing Systems (NeurIPS)*.

Yang, T.; Ren, P.; Xie, X.; and Zhang, L. 2021. GAN Prior Embedded Network for Blind Face Restoration in the Wild. In *IEEE/CVF Conference on Computer Vision and Pattern Recognition (CVPR)*, 672–681.

Ye, H.; Zhang, J.; Liu, S.; Han, X.; and Yang, W. 2023. IP-Adapter: Text Compatible Image Prompt Adapter for Text-to-Image Diffusion Models. *arXiv preprint arXiv:2308.06721*.

Yin, Z.; Chen, J.; Liu, M.; Wang, Z.; Li, F.; Pei, R.; Li, X.; Lau, R. W. H.; and Zuo, W. 2026. RefSTAR: Blind Face Image Restoration with Reference Selection, Transfer, and Reconstruction. In *Proceedings of the AAAI Conference on Artificial Intelligence*.

Ying, J.; Liu, M.; Wu, Z.; Zhang, R.; Yu, Z.; Fu, S.; Cao, S.-Y.; Wu, C.; Yu, Y.; and Shen, H.-L. 2024. RestorerID: Towards Tuning-Free Face Restoration with ID Preservation. *arXiv preprint arXiv:2411.14125*.

Zhang, H.; Alaluf, Y.; Ma, S.; Kadambi, A.; Wang, J.; and Aberman, K. 2024. InstantRestore: Single-Step Personalized Face Restoration with Shared-Image Attention. *arXiv preprint arXiv:2412.06753*.

Zhang, L.; Rao, A.; and Agrawala, M. 2023. Adding Conditional Control to Text-to-Image Diffusion Models. In *IEEE/CVF International Conference on Computer Vision (ICCV)*, 3836–3847.

Zhao, Y.; Hou, T.; Su, Y.-C.; Jia, X.; Li, Y.; and Grundmann, M. 2023. Towards Authentic Face Restoration with Iterative Diffusion Models and Beyond. In *Proceedings of the IEEE/CVF International Conference on Computer Vision (ICCV)*, 7312–7322.

Zhou, S.; Chan, K. C.; Li, C.; and Loy, C. C. 2022. Towards Robust Blind Face Restoration with Codebook Lookup Transformer. In *Advances in Neural Information Processing Systems (NeurIPS)*.

Supplementary Material for IConFace: Identity-Structure Asymmetric Conditioning for Unified Reference-Aware Face Restoration

Axi Niu*, Jinyang Zhang*, Senyan Qing

Northwestern Polytechnical University

nax@nwpu.edu.cn zhangjinyang@mail.nwpu.edu.cn qingsenyan@nwpu.edu.cn

Homepage: <https://cosmicrealm.github.io/IConFace/>

*These authors contributed equally.

Supplementary Overview

This supplement provides protocol details, implementation specifications, and diagnostic evidence supporting the main paper: (i) dataset, training, inference, comparison-method, and metric protocols; (ii) reference-GT gap statistics, target-state distortion/structure checks, and GT-AdaFace analysis; and (iii) extended reference-aware, no-reference, and ablation visual comparisons. The main paper reports the compact method and benchmark summary, while this supplement documents the implementation choices and additional quantitative/qualitative evidence behind those results.

Protocol and Implementation Details

Training data. IConFace is trained on FFHQ-Ref, a reference-aware extension of FFHQ. FFHQ contains 70,000 aligned 1024×1024 face images with broad variation in age, ethnicity, background, accessories, and image conditions. FFHQ-Ref groups FFHQ images by ArcFace-predicted identity and provides reference mappings for images that have same-identity partners. The released FFHQ-Ref reference graph contains 20,405 usable high-quality images; our training split is the trainval mapping, which contains 6,373 identity groups and 19,548 usable images with at least one same-identity reference. During training, the target image is degraded online with mixed blind degradations, while same-identity images from the mapping serve as optional protocol references.

Evaluation data. Reference-aware evaluation uses CelebA-Test-Ref, FFHQ-Ref Moderate, FFHQ-Ref Severe, and CelebHQRef100. CelebA-Test-Ref contains 2,533 test samples with paired LQ/GT images and same-identity references from CelebA-HQ/CelebAMask-HQ. FFHQ-Ref Moderate and FFHQ-Ref Severe each contain 857 FFHQ-Ref test targets with fixed same-identity references and two synthetic degradation levels. CelebHQRef100 is a compact diagnostic benchmark built from 100 high-quality identity groups. The identities are selected deterministically from the sorted source identity folders, the first sorted image is used as target/GT, up to three remaining same-identity images are used as protocol references, and the target is degraded with mixed BSRGAN and Real-ESRGAN style degradations using downsampling scales from 4 to 10. The degradation seed is fixed as $42 + i$ for identity index i to make the generated LQ images deterministic. CelebHQRef100 is not used for training, checkpoint selection,

or prompt tuning. We verified that no released CelebHQRef100 image path or protocol identity folder appears in the FFHQ-Ref trainval mapping; the split is used only as a compact diagnostic benchmark. No-reference evaluation uses CelebA-Test (3,000 paired synthetic samples), LFW (1,711), CelebChild (360), WebPhoto (407), and Wider-Test (970); LFW, CelebChild, WebPhoto, and Wider-Test are treated as real-world sets without paired ground truth.

Backbone, training, and inference. IConFace uses the FLUX.2-klein-base-4B restoration backbone and adds rank 16 LoRA adapters together with the identity and degraded-structure modules described in the main paper. The final optimization setting uses 512×512 crops, fixed learning rate $1e-5$, batch size 1, and gradient accumulation 4. Degradation strength is sampled from 0–16 with bucket probabilities 0.5, 0.3, and 0.2 for ranges 0–3, 4–8, and 9–16. All reported results use 12 sampling steps, guidance scale 4.0, base seed 42, and 512 resolution.

Reference sampling and conditioning. Training mixes reference availability so the same checkpoint can operate with or without references: 30% of samples use no reference, 30% use one, 20% use two, and 20% use three. When fewer than three references are available, we use the actual number without duplication. The global identity pathway uses AdaFace IR50 embeddings with norm-only multi-reference aggregation and temperature 1.0. The degraded structure pathway uses degraded strength 1.0 and low-rank degraded cross-attention rank 16. No-reference inference removes reference tokens and uses the degraded-image AdaFace fallback only as weak forward conditioning.

The implemented objective uses the same losses as the main paper with explicit scalar multipliers. Eq. (8) uses uniform flow-matching timestep weight, $w(\sigma) = 1$ (`loss_weighting=none`), and scalar multiplier $\alpha_{\text{fm}} = 0.75$. The AdaFace identity multiplier is $\lambda_{\text{id}} = 0.30$, the hard target stabilizer uses $\lambda_h = 0.25$, and the sigma floor is $\omega_{\text{min}} = 0.25$:

$$\mathcal{L} = \alpha_{\text{fm}} \mathcal{L}_{\text{fm}} + \lambda_{\text{id}} \omega(\sigma) [(1 - \lambda_h^*) \mathcal{L}_{\text{ref-id}} + \lambda_h^* \mathcal{L}_{\text{hard}}], \quad (1)$$

where $\lambda_h^* = \lambda_h (1 - \cos(e_{\text{ref}}, e_{\text{gt}}))$ and $\omega(\sigma) = \max(1 - \sigma, \omega_{\text{min}})^2$. Legacy sigma-threshold launcher fields are ignored by the final identity loss; the only active sigma control is the floor $\omega_{\text{min}} = 0.25$ above.

Token packing and RoPE. All image and text conditions use the four-axis FLUX.2 rotary position layout (t, h, w, l) .

Scene latents are packed from (B, C, H, W) to (B, HW, C) with ids $(0, h, w, 0)$, while text tokens use ids $(0, 0, 0, l)$. The degraded image condition is assigned a separate temporal group with $t = 2$. Reference images are packed as grouped visual tokens with $t = 10 + r$ for reference index r , which lets the transformer distinguish the generated scene, degraded observation, and each reference without changing the spatial (h, w) axes. For a token i with position id $p_i = (t_i, h_i, w_i, l_i)$, the query and key vectors are split over axes $a \in \{t, h, w, l\}$ with dimensions $d_a = [32, 32, 32, 32]$. For each two-channel pair m on axis a , the RoPE computation is

$$\omega_{a,m} = \theta^{-2m/d_a}, \quad \theta = 2000, \quad (2a)$$

$$R(\rho, \omega) = \begin{bmatrix} \cos(\rho\omega) & -\sin(\rho\omega) \\ \sin(\rho\omega) & \cos(\rho\omega) \end{bmatrix}, \quad (2b)$$

$$\tilde{q}_{i,a,m} = R(p_i^a, \omega_{a,m})q_{i,a,m}, \quad (2c)$$

$$\tilde{k}_{j,a,m} = R(p_j^a, \omega_{a,m})k_{j,a,m}, \quad (2d)$$

$$\text{Attn}_{ij} \propto \exp\left(\frac{\tilde{q}_i^\top \tilde{k}_j}{\sqrt{d}}\right). \quad (2e)$$

This construction preserves the ordinary spatial axes while using the temporal axis to mark scene, degraded, and reference token groups.

Comparison methods. Reference-aware baselines are DMDNet, ReF-LDM, RestorerID, InstantRestore, and FaceMe; they are evaluated with the same protocol references whenever supported. Blind baselines are GFP-GAN, VQFR, CodeFormer, RestoreFormer++, and DAEFR, evaluated in the empty-reference setting. DMDNet learns dual memory dictionaries; ReF-LDM uses latent diffusion with high-quality references; RestorerID injects single-reference identity through an ID-preserving adapter; InstantRestore uses shared-image attention for single-step personalized restoration; and FaceMe extracts identity prompts from references. For blind baselines, GFP-GAN uses a GAN facial prior, VQFR uses a vector-quantized dictionary, CodeFormer predicts codebook entries with a transformer, RestoreFormer++ uses reconstruction-oriented priors, and DAEFR couples LQ evidence with high-quality codebook priors. References for these methods are provided in the main paper.

Metrics. For each reference-aware sample, let \hat{I}_i be the restored image and R_i^1 be the first protocol reference. Ref-ArcFace and Ref-AdaFace are dataset averages of cosine similarities

$$\text{RefMetric} = \frac{1}{N} \sum_{i=1}^N \frac{E(\hat{I}_i)^\top E(R_i^1)}{\|E(\hat{I}_i)\|_2 \|E(R_i^1)\|_2}, \quad (3)$$

where E is the corresponding frozen ArcFace or AdaFace encoder. We also report GT-AdaFace in the analysis section as the cosine similarity between \hat{I}_i and the paired target image G_i . PSNR, SSIM, and LPIPS are computed only on paired synthetic benchmarks and are treated as target-state distortion/structure checks rather than primary real-world quality metrics. MUSIQ, CLIP-IQA, and MANIQA

are learned no-reference perceptual quality metrics; each restored image is scored independently and the dataset mean is reported. We use these metrics together so that reference-aligned identity consistency, target-state distortion, and perceptual quality can be read separately.

Table 1: Paired no-reference CelebA-Test distortion metrics. Main-paper no-reference results emphasize learned perceptual metrics; this table reports the standard paired distortion metrics for completeness.

Method	PSNR	SSIM	LPIPS
CodeFormer	25.146	0.685	0.227
GFP-GAN	25.105	0.696	0.241
VQFR	23.233	0.658	0.244
RestoreFormer++	25.313	0.685	0.226
DAEFR	22.591	0.628	0.250
IConFace	22.291	0.635	0.288

Reproducibility details. For reproducibility, we keep the restoration prompt, random seed, sampling steps, guidance scale, dataset split files, metric scripts, and checkpoint identifiers fixed across all reported evaluations. The released code package is organized around the inference and evaluation paths used for the main-paper tables and qualitative panels.

Reference-Aligned Identity Metric Analysis

Reference-aware restoration has two identity-related observations: the degraded target image, whose clean counterpart defines the target state, and one or more same-identity references, which provide external identity evidence. These observations are not spatially aligned and may differ in pose, expression, illumination, age, makeup, occlusion, or local facial state. Therefore, a GT-aligned identity score and a reference-aligned identity score do not always measure the same property. GT-aligned identity measures resemblance to the target-state image, while Ref-ArcFace and Ref-AdaFace measure consistency with the fixed reference evidence supplied by the protocol.

This distinction is important for interpreting reference-aware results. If the reference and GT are nearly identical, GT-based and reference-based identity scores tend to agree. When the reference and GT are only moderately aligned, however, a GT-only score can penalize a restoration that correctly uses reference identity evidence but does not reproduce the exact target-state appearance. We therefore treat Ref-AdaFace as the primary reference-aware identity metric, report perceptual quality metrics alongside it, and use qualitative comparisons to verify that the restored face still follows the degraded-image structure rather than copying the reference pose or expression.

Table 2: Identity similarity between the first protocol reference and the GT target over the full reference-aware evaluation splits. The last three columns report the percentage of samples whose Ref₁-GT AdaFace similarity falls below each threshold.

Dataset	N	Ref ₁ -GT ArcFace	Ref ₁ -GT AdaFace	AdaFace < 0.5	AdaFace < 0.6	AdaFace < 0.7
CelebA-Test-Ref	2533	0.616±0.093	0.605±0.104	15.52%	49.11%	80.77%
FFHQ-Ref Moderate	857	0.687±0.084	0.663±0.099	4.55%	23.45%	63.36%
FFHQ-Ref Severe	857	0.687±0.084	0.663±0.099	4.55%	23.45%	63.36%
CelebHQRef100	100	0.653±0.107	0.640±0.113	16.00%	34.00%	73.00%

Table 3: Paired target-state checks on the reference-aware benchmarks. SSIM is the direct structure check; PSNR and LPIPS give distortion context.

Dataset	Method	PSNR	SSIM	LPIPS
CelebA-Test-Ref	DMDNet	25.535	0.696	0.253
	ReF-LDM	23.901	0.638	0.268
	RestorerID	24.744	0.662	0.279
	InstantRestore	25.400	0.702	0.219
	FaceMe	25.947	0.698	0.253
	IConFace	22.327	0.632	0.277
FFHQ-Ref Moderate	DMDNet	25.844	0.726	0.234
	ReF-LDM	23.971	0.664	0.232
	RestorerID	24.924	0.691	0.240
	InstantRestore	25.452	0.727	0.213
	FaceMe	26.335	0.733	0.173
	IConFace	22.755	0.671	0.218
FFHQ-Ref Severe	DMDNet	20.111	0.570	0.449
	ReF-LDM	19.563	0.566	0.347
	RestorerID	19.412	0.559	0.415
	InstantRestore	21.372	0.647	0.323
	FaceMe	20.606	0.616	0.338
	IConFace	18.376	0.570	0.357
CelebHQRef100	DMDNet	22.857	0.648	0.304
	ReF-LDM	21.701	0.615	0.289
	RestorerID	21.857	0.612	0.340
	InstantRestore	22.801	0.674	0.244
	FaceMe	22.598	0.659	0.307
	IConFace	20.479	0.627	0.283

Table 2 shows that reference-GT mismatch is common. The FFHQ-Ref rows are identical because the Moderate and Severe splits share the same GT/reference protocol and differ only in degraded inputs. CelebA-Test-Ref is clearest: 49.11% and 80.77% of Ref₁-GT pairs fall below AdaFace 0.6 and 0.7. This is not a protocol error; reference and GT images are same-identity portraits captured under different pose, expression, lighting, age, makeup, occlusion, or local facial states. A reference-aware result can therefore become more consistent with supplied identity evidence without exactly reproducing the paired target state. The diagnostic panels in Figures 1-4 verify the complementary requirement: IConFace improves identity cues such as facial geometry, eye spacing, nose/mouth shape, and local identity marks, while pose, expression, and layout remain anchored to the degraded target rather than copied from the reference.

Table 3 provides paired target-state checks. IConFace has the lowest PSNR on these benchmarks, consistent with the perception-distortion tradeoff of Blau and Michaeli (2018): a flow/diffusion-style restorer that recovers plausible identity-consistent detail is not optimized for pixel-wise regression to the paired GT. The tradeoff is metric-dependent.

Table 4: GT-AdaFace on the full reference-aware benchmarks. Scores are computed against paired GT targets rather than protocol references.

Method	CelebA	FFHQ-M	FFHQ-S	CHQ100
DMDNet	0.768	0.835	0.170	0.509
ReF-LDM	0.806	0.862	0.661	0.683
RestorerID	0.782	0.828	0.412	0.543
InstantRestore	0.797	0.841	0.551	0.664
FaceMe	0.826	0.894	0.546	0.582
IConFace	0.736	0.814	0.717	0.712

On FFHQ-Ref Severe, IConFace has lower PSNR but better LPIPS than DMDNet and RestorerID and close LPIPS to ReF-LDM. SSIM is competitive on FFHQ-Ref Moderate/Severe and CelebHQRef100, while the CelebA-Test-Ref gap reflects the high Ref₁-GT divergence rate on that benchmark (Table 2), where reference-guided restoration can legitimately deviate from the exact target-state pixel structure. Table 1 gives the analogous paired CelebA-Test blind metrics. Together with the main-paper MUSIQ/CLIP-IQA/MANIQA results, these checks show an identity-perception/distortion tradeoff rather than a PSNR-oriented optimization.

Table 4 makes the GT-based identity picture explicit. The reversal is the key observation: IConFace is not highest on GT-AdaFace in the easier CelebA-Test-Ref and FFHQ-Ref Moderate splits, but becomes strongest on FFHQ-Ref Severe and CelebHQRef100. This directly validates the asymmetric design intent. When the degraded input retains sufficient identity evidence, the reference anchor can introduce mild divergence from the specific target state if Ref₁ and GT differ; conservative baselines may therefore stay closer to the paired GT. When severe degradation destroys that evidence, the reference pathway provides the reliable identity signal, and both Ref-AdaFace and GT-AdaFace improve. Thus high Ref-AdaFace is meaningful only when read together with GT identity, structure checks, and visual evidence that the output keeps the degraded pose/expression rather than copying the reference.

Qualitative material. The following pages expand the qualitative evidence for each benchmark. Reference-aware figures report AdaFace similarity to the first protocol reference image, while no-reference pages omit identity scores because no same-identity reference is supplied. The selected reference-GT diagnostic cases are drawn from the 20 lowest IConFace GT-AdaFace cases in each split and kept when Ref₁ and GT show a visible facial-state gap with clear inter-method differences; the Ref₁ and GT columns expose the actual Ref₁-GT AdaFace values.

CelebA-Test-Ref selected reference-GT gap cases

Ref ₁	LQ	DMD Net	ReF- LDM	RestorerID	Instant Restore	FaceMe	Ours	GT
GT 0.459 R1 1.000	GT 0.454 R1 0.213	GT 0.450 R1 0.228	GT 0.509 R1 0.447	GT 0.568 R1 0.291	GT 0.617 R1 0.215	GT 0.534 R1 0.225	GT 0.351 R1 0.590	GT 1.000 R1 0.459
GT 0.512 R1 1.000	GT 0.730 R1 0.360	GT 0.740 R1 0.314	GT 0.716 R1 0.482	GT 0.636 R1 0.473	GT 0.795 R1 0.400	GT 0.794 R1 0.503	GT 0.478 R1 0.651	GT 1.000 R1 0.512
GT 0.573 R1 1.000	GT 0.711 R1 0.476	GT 0.688 R1 0.469	GT 0.696 R1 0.640	GT 0.651 R1 0.438	GT 0.727 R1 0.498	GT 0.775 R1 0.555	GT 0.498 R1 0.813	GT 1.000 R1 0.573
GT 0.351 R1 1.000	GT 0.778 R1 0.247	GT 0.733 R1 0.271	GT 0.705 R1 0.295	GT 0.602 R1 0.299	GT 0.541 R1 0.251	GT 0.790 R1 0.359	GT 0.436 R1 0.559	GT 1.000 R1 0.351

Figure 1: CelebA-Test-Ref reference-GT gap cases. Scores are AdaFace to GT/R1; the final row is an added low Ref₁-GT case. IDs: 18646, 20257, 26060, 02060.

FFHQ-Ref-Moderate selected reference-GT gap cases

Ref ₁	LQ	DMD Net	ReF- LDM	RestorerID	Instant Restore	FaceMe	Ours	GT
GT 0.509 R1 1.000	GT 0.834 R1 0.495	GT 0.865 R1 0.442	GT 0.739 R1 0.432	GT 0.818 R1 0.486	GT 0.780 R1 0.427	GT 0.843 R1 0.464	GT 0.592 R1 0.663	GT 1.000 R1 0.509
GT 0.469 R1 1.000	GT 0.548 R1 0.250	GT 0.530 R1 0.200	GT 0.683 R1 0.372	GT 0.607 R1 0.341	GT 0.759 R1 0.313	GT 0.644 R1 0.355	GT 0.607 R1 0.536	GT 1.000 R1 0.469
GT 0.479 R1 1.000	GT 0.942 R1 0.515	GT 0.946 R1 0.487	GT 0.873 R1 0.450	GT 0.917 R1 0.485	GT 0.885 R1 0.414	GT 0.942 R1 0.557	GT 0.642 R1 0.729	GT 1.000 R1 0.479
GT 0.296 R1 1.000	GT 0.613 R1 0.148	GT 0.678 R1 0.113	GT 0.637 R1 0.221	GT 0.640 R1 0.139	GT 0.634 R1 0.238	GT 0.765 R1 0.197	GT 0.658 R1 0.365	GT 1.000 R1 0.296

Figure 2: FFHQ-Ref-Moderate reference-GT gap cases. Scores are AdaFace to GT/R1; the final row is an added low Ref₁-GT case. IDs: 57244, 31223, 02293, 37245.

FFHQ-Ref-Severe selected reference-GT gap cases

Ref ₁	LQ	DMD Net	ReF- LDM	RestorerID	Instant Restore	FaceMe	Ours	GT
GT 0.369	GT -0.003	GT 0.179	GT 0.469	GT 0.335	GT 0.331	GT 0.455	GT 0.450	GT 1.000
R1 1.000	R1 -0.039	R1 0.126	R1 0.321	R1 0.412	R1 0.195	R1 0.313	R1 0.468	R1 0.369
GT 0.513	GT 0.060	GT 0.018	GT 0.492	GT 0.456	GT 0.336	GT 0.462	GT 0.473	GT 1.000
R1 1.000	R1 0.113	R1 0.099	R1 0.379	R1 0.368	R1 0.222	R1 0.359	R1 0.705	R1 0.513
GT 0.449	GT 0.357	GT 0.155	GT 0.538	GT 0.398	GT 0.604	GT 0.645	GT 0.483	GT 1.000
R1 1.000	R1 0.160	R1 0.093	R1 0.415	R1 0.217	R1 0.456	R1 0.424	R1 0.724	R1 0.449
GT 0.416	GT 0.131	GT 0.048	GT 0.491	GT 0.292	GT 0.402	GT 0.325	GT 0.484	GT 1.000
R1 1.000	R1 0.054	R1 0.028	R1 0.457	R1 0.344	R1 0.315	R1 0.231	R1 0.584	R1 0.416

Figure 3: FFHQ-Ref-Severe reference-GT gap cases. Scores are AdaFace to GT/R1; the final row is an added low Ref₁-GT case. IDs: 48700, 04716, 12051, 08081.

CelebHQRef100 selected reference-GT gap cases

Ref ₁	LQ	DMD Net	ReF- LDM	RestorerID	Instant Restore	FaceMe	Ours	GT
GT 0.395	GT -0.006	GT 0.032	GT 0.335	GT -0.008	GT 0.358	GT 0.201	GT 0.406	GT 1.000
R1 1.000	R1 -0.040	R1 -0.001	R1 0.348	R1 -0.003	R1 0.279	R1 0.174	R1 0.642	R1 0.395
GT 0.554	GT 0.380	GT 0.461	GT 0.574	GT 0.547	GT 0.575	GT 0.571	GT 0.489	GT 1.000
R1 1.000	R1 0.212	R1 0.352	R1 0.586	R1 0.426	R1 0.519	R1 0.482	R1 0.618	R1 0.554
GT 0.683	GT 0.027	GT 0.489	GT 0.458	GT 0.151	GT 0.349	GT 0.180	GT 0.515	GT 1.000
R1 1.000	R1 0.024	R1 0.535	R1 0.293	R1 0.108	R1 0.286	R1 0.120	R1 0.680	R1 0.683
GT 0.414	GT -0.051	GT 0.082	GT 0.516	GT 0.193	GT 0.482	GT 0.291	GT 0.502	GT 1.000
R1 1.000	R1 -0.015	R1 -0.029	R1 0.540	R1 0.144	R1 0.267	R1 0.214	R1 0.683	R1 0.414

Figure 4: CelebHQRef100 reference-GT gap cases. Scores are AdaFace to GT/R1; the final row is an added low Ref₁-GT case. IDs: 00051_0, 00074_0, 00090_0, 00072_0.

CelebA-Test-Ref

Ref	LQ	DMDNet	ReF-LDM	RestorerID	InstantRestore	FaceMe	Ours	GT
CelebA-Test-Ref: case 18646								
1.000	0.213	0.228	0.447	0.291	0.215	0.225	0.590	0.459
CelebA-Test-Ref: case 24093								
1.000	0.293	0.306	0.338	0.255	0.307	0.309	0.422	0.380
CelebA-Test-Ref: case 17353								
1.000	0.195	0.173	0.272	0.394	0.222	0.343	0.567	0.389
CelebA-Test-Ref: case 27315								
1.000	0.235	0.269	0.513	0.479	0.494	0.488	0.577	0.448
CelebA-Test-Ref: case 02060								
1.000	0.247	0.271	0.295	0.299	0.251	0.359	0.559	0.351
CelebA-Test-Ref: case 18375								
1.000	0.273	0.319	0.395	0.461	0.514	0.526	0.569	0.465
CelebA-Test-Ref: case 19681								
1.000	0.212	0.126	0.323	0.248	0.182	0.257	0.535	0.388
CelebA-Test-Ref: case 08806								
1.000	0.296	0.232	0.413	0.430	0.316	0.401	0.506	0.515
CelebA-Test-Ref: case 20257								
1.000	0.360	0.314	0.482	0.473	0.400	0.503	0.651	0.512
CelebA-Test-Ref: case 00218								
1.000	0.323	0.346	0.361	0.419	0.366	0.386	0.430	0.469

Figure 5: Additional reference-aware qualitative comparisons on CelebA-Test-Ref. Scores under images report AdaFace similarity to the first protocol reference.

FFHQ-Ref-Moderate
























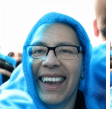
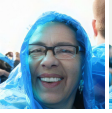






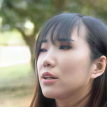














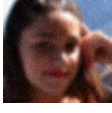
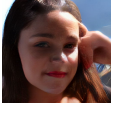

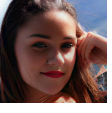
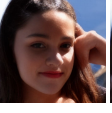
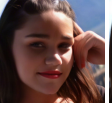


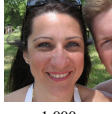
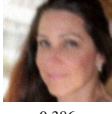
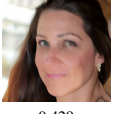

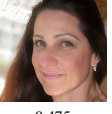
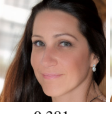
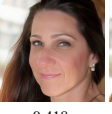
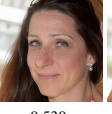












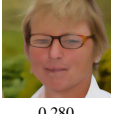






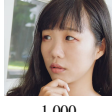
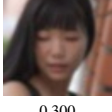
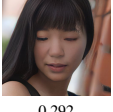

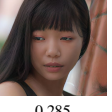
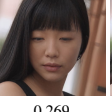
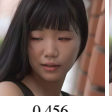
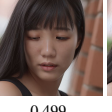

Ref	LQ	DMDNet	ReF-LDM	RestorerID	InstantRestore	FaceMe	Ours	GT
FFHQ-Ref-Moderate: case 57244								
								
1.000	0.495	0.442	0.432	0.486	0.427	0.464	0.663	0.509
FFHQ-Ref-Moderate: case 44570								
								
1.000	0.374	0.224	0.356	0.366	0.478	0.470	0.593	0.533
FFHQ-Ref-Moderate: case 55156								
								
1.000	0.315	0.322	0.436	0.363	0.356	0.447	0.671	0.541
FFHQ-Ref-Moderate: case 48700								
								
1.000	0.262	0.242	0.400	0.318	0.306	0.360	0.439	0.369
FFHQ-Ref-Moderate: case 54575								
								
1.000	0.521	0.523	0.587	0.455	0.536	0.586	0.628	0.610
FFHQ-Ref-Moderate: case 31223								
								
1.000	0.250	0.200	0.372	0.341	0.313	0.355	0.536	0.469
FFHQ-Ref-Moderate: case 08081								
								
1.000	0.386	0.429	0.471	0.475	0.381	0.418	0.530	0.416
FFHQ-Ref-Moderate: case 27262								
								
1.000	0.346	0.177	0.507	0.461	0.479	0.530	0.595	0.519
FFHQ-Ref-Moderate: case 15716								
								
1.000	0.376	0.280	0.536	0.381	0.428	0.488	0.590	0.488
FFHQ-Ref-Moderate: case 02647								
								
1.000	0.300	0.292	0.362	0.285	0.269	0.456	0.499	0.400

Figure 6: Additional reference-aware qualitative comparisons on FFHQ-Ref Moderate. Scores under images report AdaFace similarity to the first protocol reference.

FFHQ-Ref-Severe

Ref	LQ	DMDNet	ReF-LDM	RestorerID	InstantRestore	FaceMe	Ours	GT
FFHQ-Ref-Severe: case 02647								
1.000	0.206	0.205	0.491	0.323	0.407	0.373	0.520	0.400
FFHQ-Ref-Severe: case 17083								
1.000	0.309	0.153	0.410	0.381	0.409	0.407	0.515	0.513
FFHQ-Ref-Severe: case 04716								
1.000	0.113	0.099	0.379	0.368	0.222	0.359	0.705	0.513
FFHQ-Ref-Severe: case 12051								
1.000	0.160	0.093	0.415	0.217	0.456	0.424	0.724	0.449
FFHQ-Ref-Severe: case 48700								
1.000	-0.039	0.126	0.321	0.412	0.195	0.313	0.468	0.369
FFHQ-Ref-Severe: case 14836								
1.000	0.050	0.094	0.555	0.239	0.493	0.326	0.739	0.596
FFHQ-Ref-Severe: case 27211								
1.000	0.082	0.136	0.538	0.465	0.353	0.491	0.464	0.416
FFHQ-Ref-Severe: case 01829								
1.000	0.028	0.042	0.637	0.441	0.485	0.359	0.653	0.518
FFHQ-Ref-Severe: case 02293								
1.000	0.061	0.160	0.556	0.487	0.324	0.492	0.843	0.479
FFHQ-Ref-Severe: case 69793								
1.000	0.028	0.104	0.508	0.289	0.316	0.253	0.724	0.521

Figure 7: Additional reference-aware qualitative comparisons on FFHQ-Ref Severe. Scores under images report AdaFace similarity to the first protocol reference.

CelebHQRef100


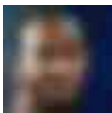



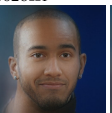
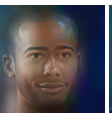
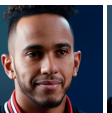




















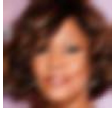







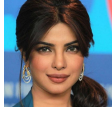
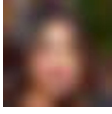
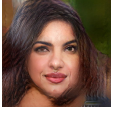


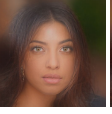
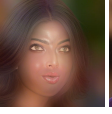
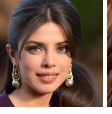











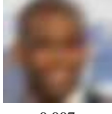
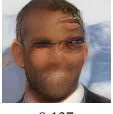


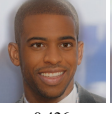





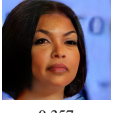




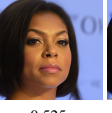

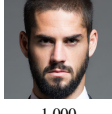
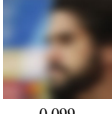
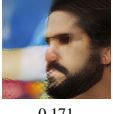
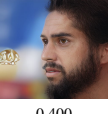
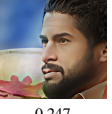
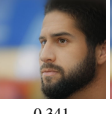
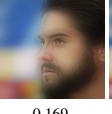
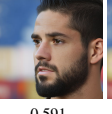


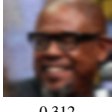







Ref	LQ	DMDNet	ReF-LDM	RestorerID	InstantRestore	FaceMe	Ours	GT
CelebHQRef100: case 00026_1								
								
1.000	0.022	0.134	0.235	0.304	0.214	0.244	0.492	0.426
CelebHQRef100: case 00098_0								
								
1.000	0.161	0.211	0.156	0.357	0.300	0.267	0.558	0.434
CelebHQRef100: case 00074_0								
								
1.000	0.212	0.352	0.586	0.426	0.519	0.482	0.618	0.554
CelebHQRef100: case 00046_1								
								
1.000	0.147	0.098	0.509	0.584	0.518	0.341	0.672	0.453
CelebHQRef100: case 00090_0								
								
1.000	0.024	0.535	0.293	0.108	0.286	0.120	0.680	0.683
CelebHQRef100: case 00067_0								
								
1.000	0.043	0.079	0.261	0.305	0.329	0.251	0.547	0.593
CelebHQRef100: case 00032_0								
								
1.000	0.007	0.137	0.447	0.428	0.426	0.216	0.620	0.488
CelebHQRef100: case 00052_0								
								
1.000	0.369	0.357	0.423	0.482	0.496	0.406	0.525	0.483
CelebHQRef100: case 00006_1								
								
1.000	0.099	0.171	0.400	0.247	0.341	0.169	0.591	0.582
CelebHQRef100: case 00049_1								
								
1.000	0.312	0.300	0.359	0.273	0.368	0.396	0.492	0.440

Figure 8: Additional reference-aware qualitative comparisons on CelebHQRef100. Scores under images report AdaFace similarity to the first protocol reference.

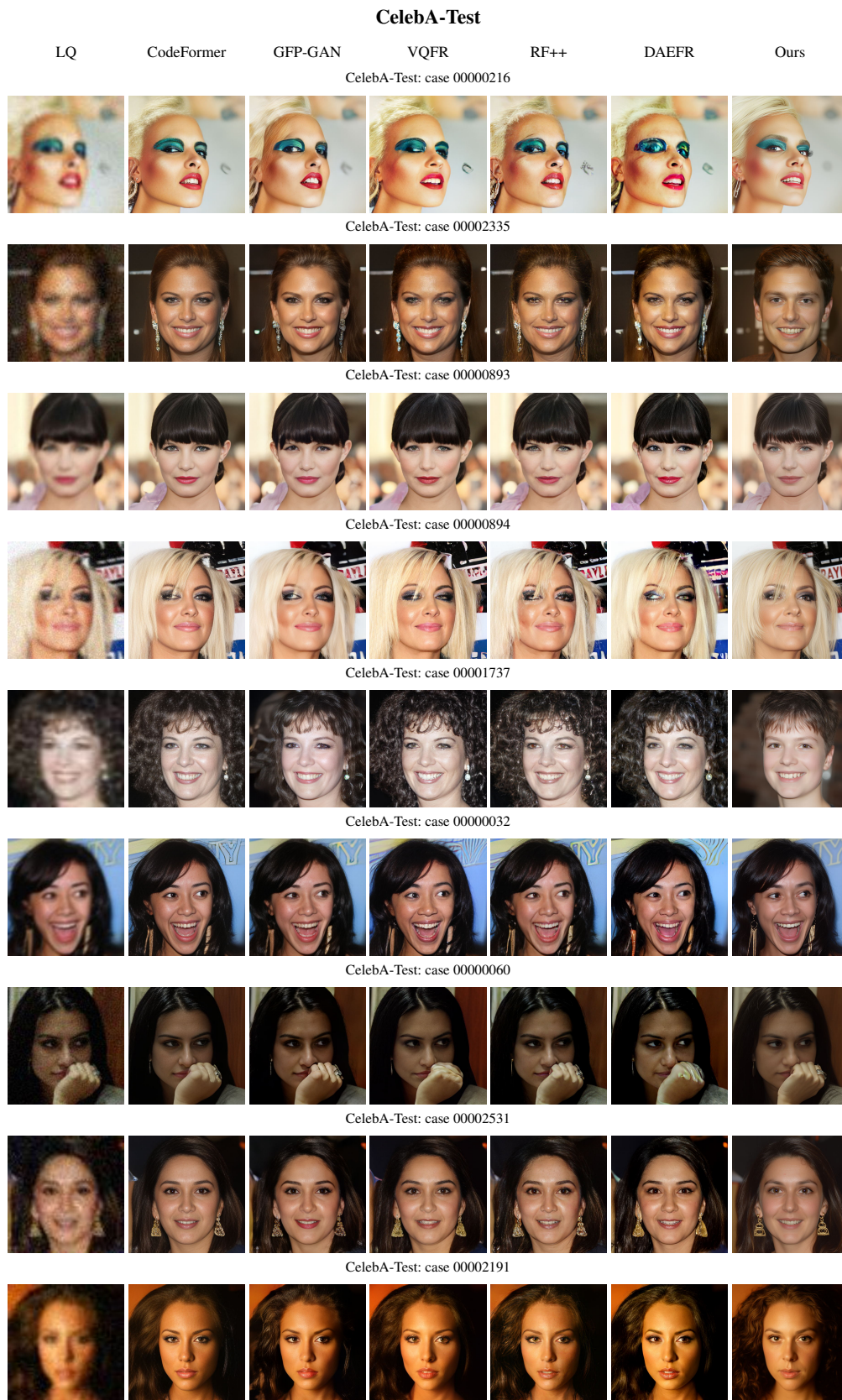


Figure 9: Additional no-reference qualitative comparisons on CelebA-Test.

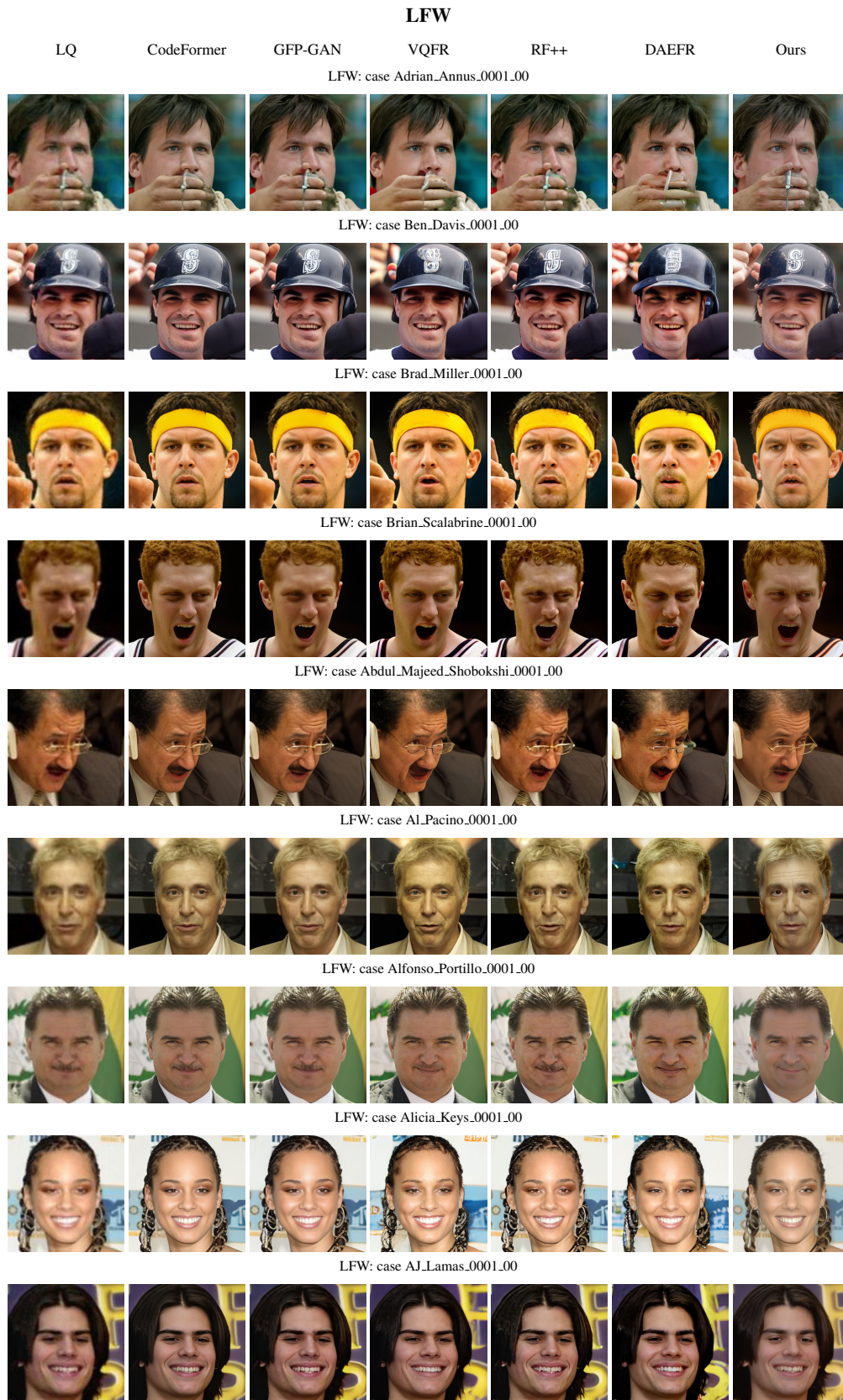


Figure 10: Additional no-reference qualitative comparisons on LFW.

CelebChild



Figure 11: Additional no-reference qualitative comparisons on CelebChild.



Figure 12: Additional no-reference qualitative comparisons on WebPhoto.

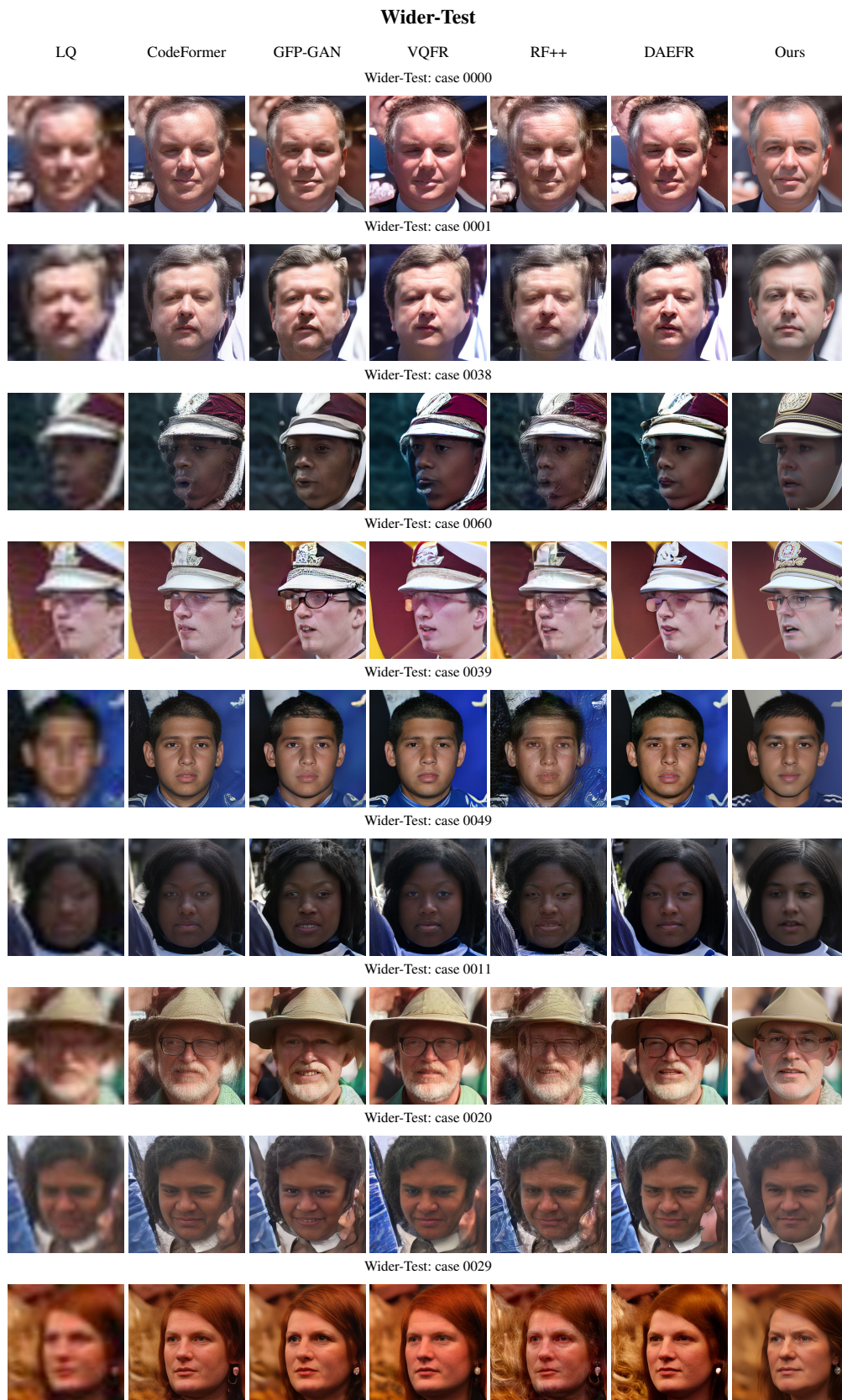


Figure 13: Additional no-reference qualitative comparisons on Wider-Test.

Reference-aware ablation (CelebHQRef100)

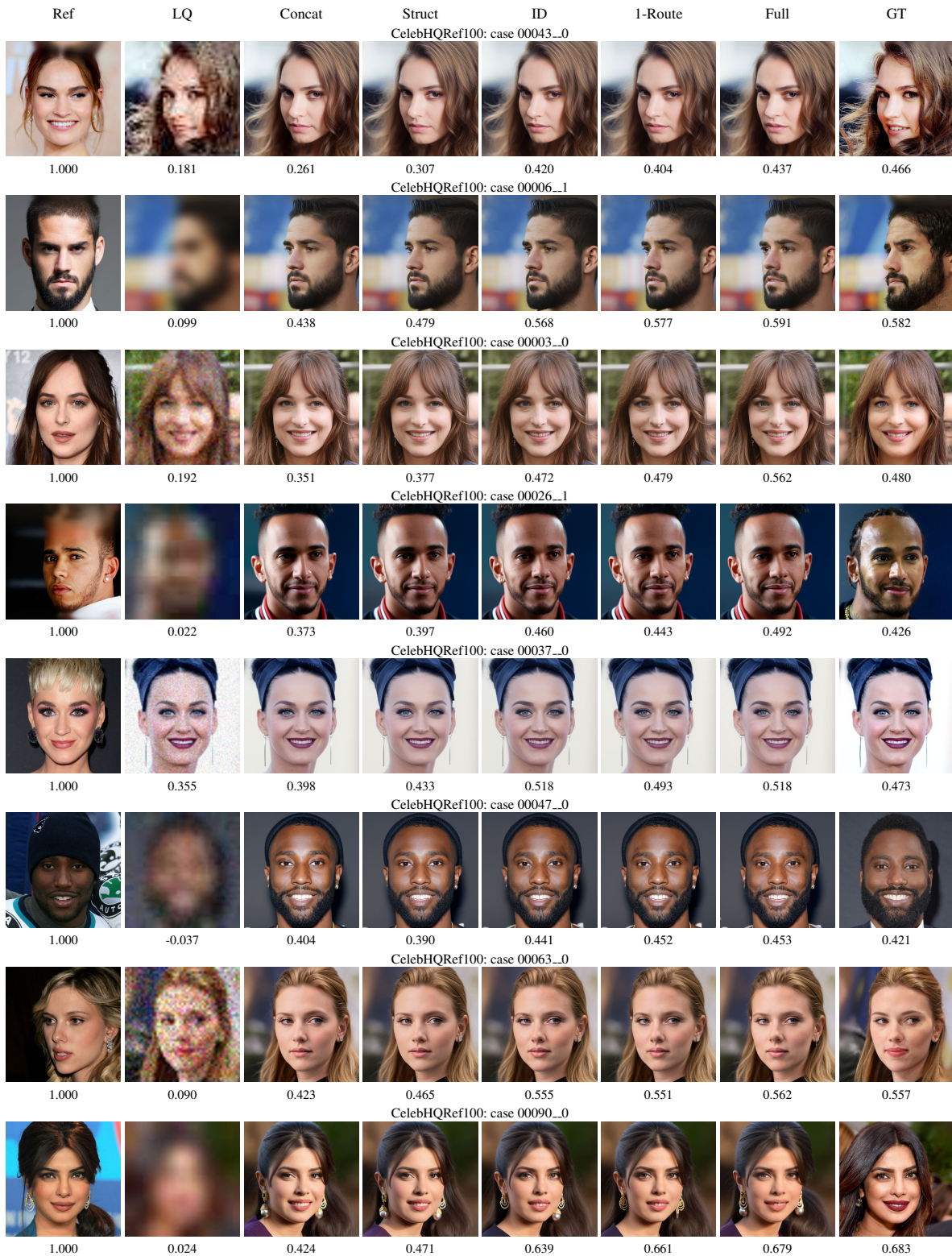


Figure 14: Reference-aware qualitative ablation on CelebHQRef100. Scores under images report AdaFace similarity to the first protocol reference.

Reference-aware ablation (FFHQ-Ref-Moderate)

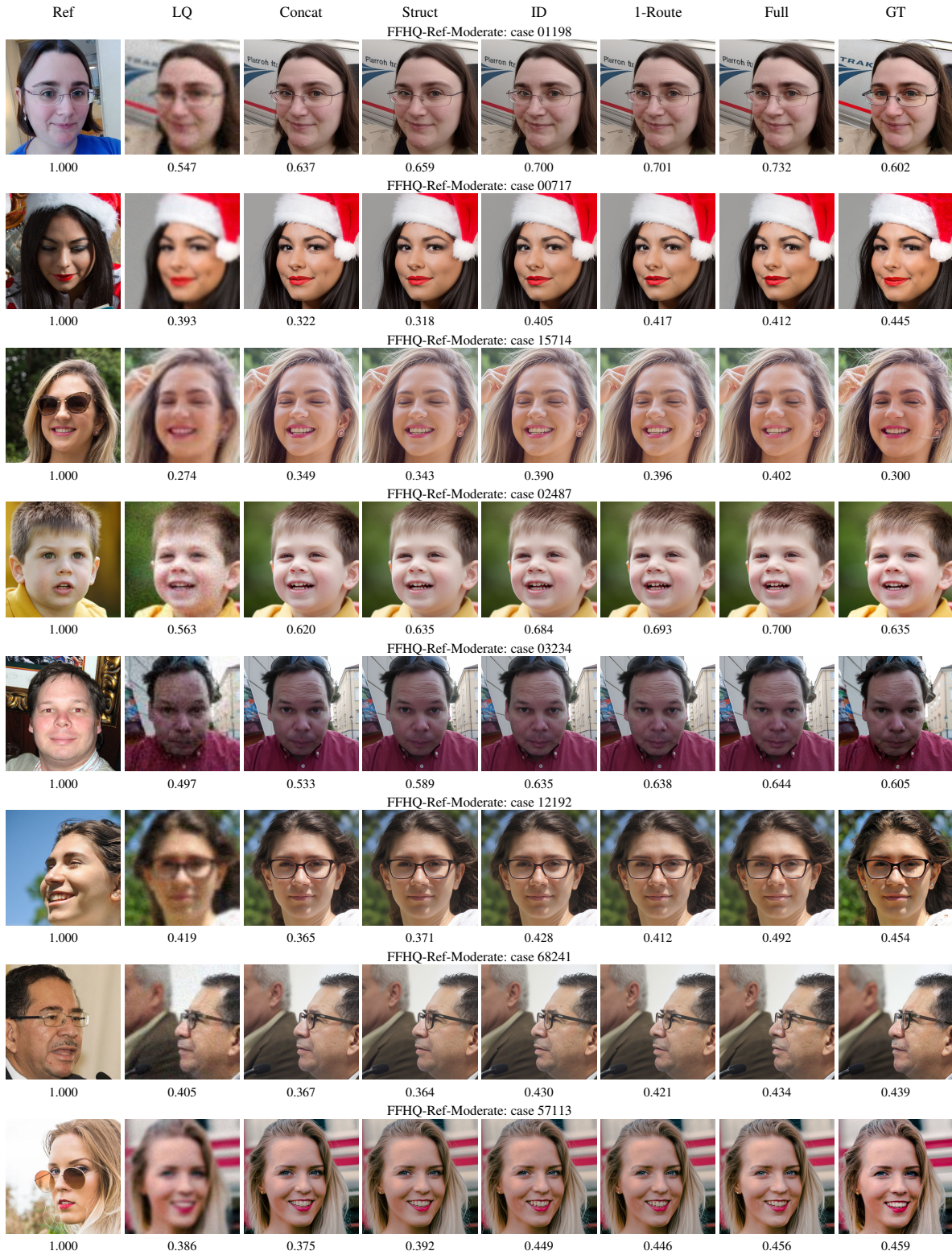


Figure 15: Reference-aware qualitative ablation on FFHQ-Ref Moderate. Scores under images report AdaFace similarity to the first protocol reference.

Reference-aware ablation (FFHQ-Ref-Severe)

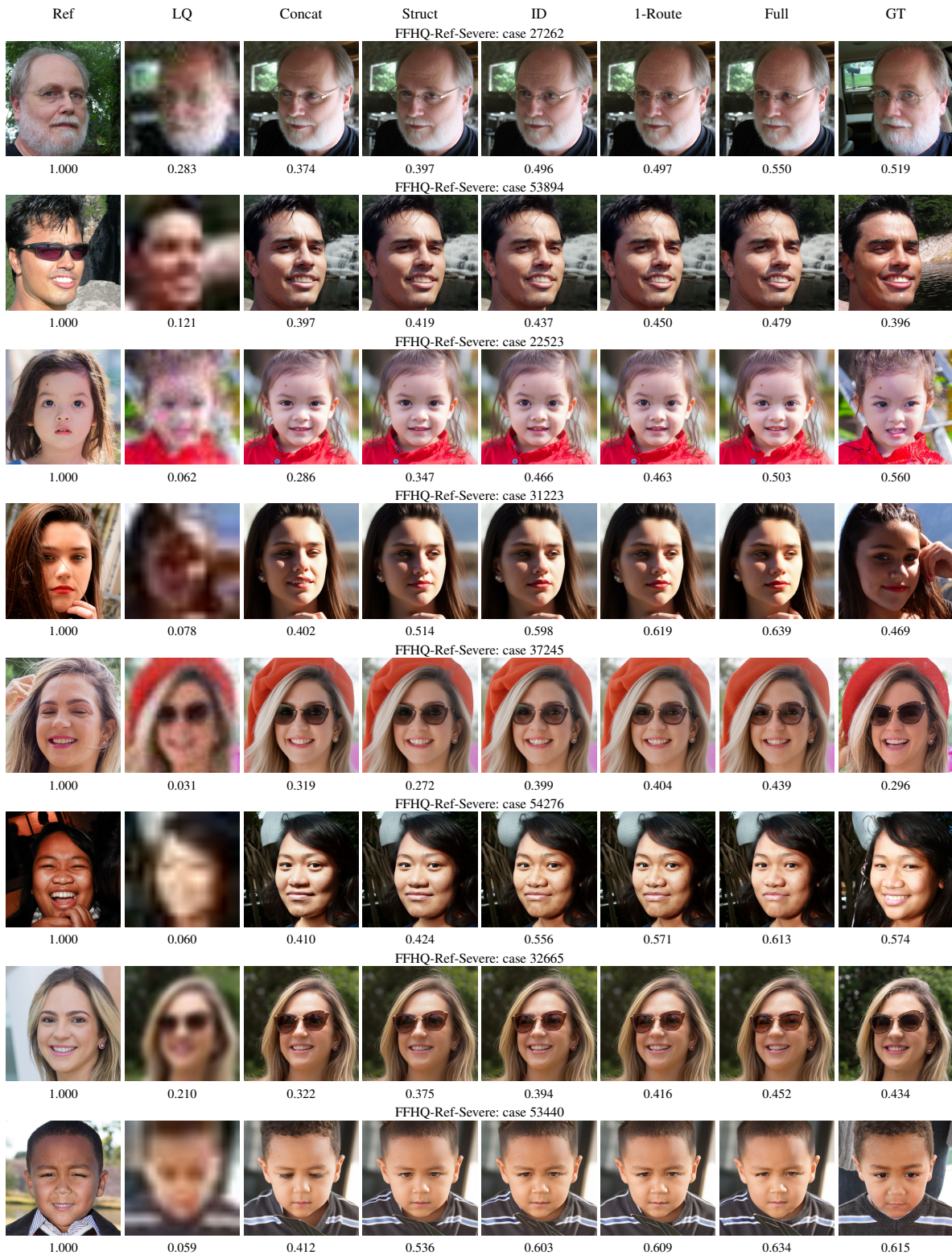


Figure 16: Reference-aware qualitative ablation on FFHQ-Ref Severe. Scores under images report AdaFace similarity to the first protocol reference.